Los Alamos
NATIONAL LABORATORY
EST. 1943

LA-UR-21-24028
Approved for public release; distribution is unlimited.

Title: Thermal Evaluation of the SAVY-4000 1 Quart Container at High Heat Loads

Author(s): Oka, Jude M.
Stone, Timothy Amos
Root, Margaret A.
Riglin, Jacob Daniel

Intended for: Report

Issued: 2021-04-27

Disclaimer:
Los Alamos National Laboratory, an affirmative action/equal opportunity employer, is operated by Triad National Security, LLC for the National Nuclear Security Administration of U.S. Department of Energy under contract 89233218CNA000001. By approving this article, the publisher recognizes that the U.S. Government retains nonexclusive, royalty-free license to publish or reproduce the published form of this contribution, or to allow others to do so, for U.S. Government purposes. Los Alamos National Laboratory requests that the publisher identify this article as work performed under the auspices of the U.S. Department of Energy. Los Alamos National Laboratory strongly supports academic freedom and a researcher's right to publish; as an institution, however, the Laboratory does not endorse the viewpoint of a publication or guarantee its technical correctness.

Thermal Evaluation of the SAVY-4000 1 Quart Container at High Heat Loads

Jude Oka[*], Tim Stone[*], Margaret Root[+], Jacob Riglin[×]

[*]ORI-2
[+]NEN-1
[×]E-1

Los Alamos National Laboratory

Table of Contents

List of Tables and Figures

Introduction

The SAVY-4000 Safety Analysis Report (SAR) was published in 2013 which established the design life of the container series through physical testing that meets applicable requirements from DOE M 441.1-1, *Nuclear Material Packaging Manual* [1,2]. One critical requirement in DOE M 441.1-1 is to set a maximum heat load for the entire series to ensure that throughout the lifetime of the container, each of the components still performs within manufacture specifications. The original maximum decay heat limit has been defined within the SAVY-4000 SAR, which was accomplished by completing a series of tests that heat loaded the SAVY-4000 series and measured the steady state temperature and graded it against manufacture specifications. The container series is comprised of a corrosion resistant 316L stainless steel containment boundary, ceramic composite filter for the prevention of radiological particulate release and a chemically stable O-ring made of Viton® [2]. Currently, the SAVY 4000 maximum decay heat load is set at 25 Watts and the heat load expected during normal handling and storage is considered sufficient that the SAVY 4000 container requirements will not be the limiting factor for storage of most common material in use at TA-55, e.g. weapons grade oxide, americium, Pu-238 oxide and encapsulated heat sources. The SAVY 4000 lifetime was originally set as 5 years within the SAVY-4000 SAR, but in July 2019 the lifetime was extended to 15 years through a technical basis justification approved by the Department of Energy (DOE) Los Alamos Field Office [3]. The 25 Watt limit applies to all SAVY 4000 container sizes; 1-quart, 2-quart, 3-quart, 5-quart, 8-quart, 12-quart, 5-gallon, and 10-gallon.

Objective

The objective of this analysis to investigate the thermal loading beyond the 25 Watt limit and to measure the steady state temperatures at various locations on the container body and key components, such as the filter and Viton O-ring. The test series will use the 1 quart SAVY-4000 container as the basis for the investigation due to its relatively small volume where it will be viewed as the conservative bounding case for all other sizes. The conclusion of the analysis will be the basis for inclusion of various Pu-238 heat sources above 25 Watts or packaging multiple heat sources into a single container that can also be above 25 Watts, yet will maintain container integrity.

Testing methods and modeling efforts

Physical testing and thermal modeling were used to investigate the 1 quart SAVY-4000 at higher heat loads beyond 25 Watts. The physical testing provides data that will provide insight into the containers components' performance at higher heat loads and will also be used to validate the thermal model. The model can then be used to investigate other sizes or container configurations not captured by physical testing. Testing was conducted at the TA-35 building 002 high bay, in conjunction with members of the NEN-1 group, while thermal modeling was completed through a collaborating effort with members of the E-1 group.

Testing was conducted using electric bullet heaters to emulate heat source plutonium and thermocouples for temperature measurements at steady state. Four different scenarios were utilized to bound high wattage source packaging configurations within the SAVY-4000 series. Thermal modeling was completed using ANSYS, which is a multiphysics engineering simulation software that is used for numerical prediction of temperatures for a given test setup. ANSYS has been used in several other projects in the past with containers such as the Pipe Overpack Container (POC) configured within a Type A 55 gallon drum for thermal analysis at high heat loads and has been proven to be a powerful tool for

thermal predictions. The model can be used for future work on temperature predictions for other SAVY-4000 sizes while introducing new configurations that have not been considered through testing.

Experimental Setup

All thermal steady-state testing was conducted on a single 1 quart SAVY-4000 container with 4 configurations to bound all high-heat-loaded configured packages to date. The configurations are as follows; bullet heaters placed within an aluminum block for stability to act as a point load, copper mesh around the bullet heater to better distribute the heat for a realistic thermal load distribution, the implementation of Manganin wire to better distribute the heat within the copper mesh and lastly, copper mesh underneath the bullet heater to force the bullet heater up against the underside of the lid. All four scenarios will be used to analyze the temperature profiles at the container's key components such as the filter, O-ring and the temperature gradient along the body wall. Temperature measurements were obtained by seven Omega K-type ready-made insulated thermocouples with glass braid insulation (Model SC-GG-K-30-36) [4]. An Omega 8-Input Portable Thermometer was used to record the temperatures measured by the thermocouples [5].

To ensure that the thermocouples were accurately calibrated to each other and to another calibrated thermometer, all 7 thermocouples and the thermometer were connected to an Al plate, see Figure 1 below. Their temperatures were recorded after 10 minutes and again after 24 hours.

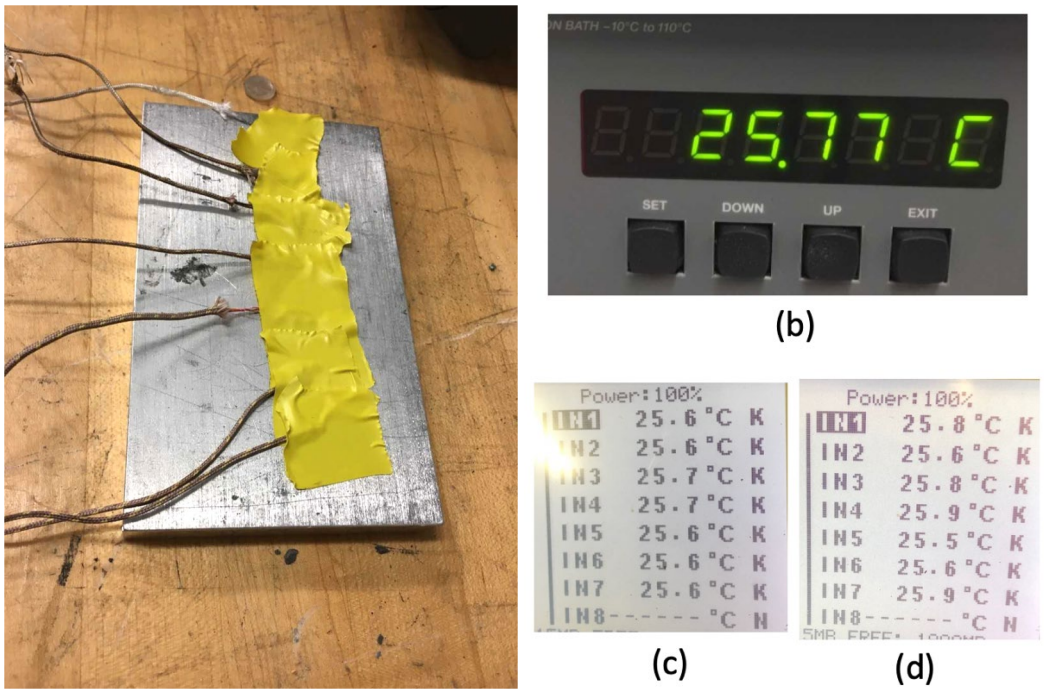

Figure 1 Thermocouple calibration measurement (a) All thermocouples attached to a single Al block. (b) Calibrated thermometer measurement of room temperature near the Al block. (c) Thermocouple readings 10 minutes after thermocouple attachment. (d) Thermocouple readings 24 hours after attachment.

The thermocouple measurements showed strong agreement within themselves and the calibrated thermometer measurement. After 10 minutes, all temperature measurements fell within +/- 0.3 °C of

one another and the calibrated thermometer measurement. After 24 hours, the thermocouple measurements fell within +/- 0.4 °C of one another. The measurements fall well within the Omega thermometer data sheet's listed uncertainty of +/- 1.0 °C. [2]. There was only a slight difference in measurement after 24 hours of baseline testing, therefore the thermocouples are considered to be operating within the manufacturers calibration.

The testing was conducted within NEN-1's high bay testing facility at TA-35. Testing was reviewed by NEN-1 management and approved to perform high wattage testing without combustible loading. The surrounding setup consisted of a high temperature welding table (to ensure that the heat did not pose a risk of fire), cement block to seat the container and to provide an adiabatic boundary, two Tempco Hi-Density Cartridge Heaters [6], seven thermocouples (three outside of the can, one on Al block, one on O-ring, one on lid filter, one air temperature), copper packing, high-temperature putty to connect thermocouples to the can, 8-input portable thermometer with a data logger and a benchtop power supply. Figure 2 below shows the setup in its entirety.

Figure 2 Entire experiment setup including the welding table, the SAVY can and the diagnostic electronics.

Figure 3 below show the images of the wire connections from the cartridge heaters to the benchtop power supply, the portable thermometer and data logger leading to the thermocouples with the laptop for measurement display.

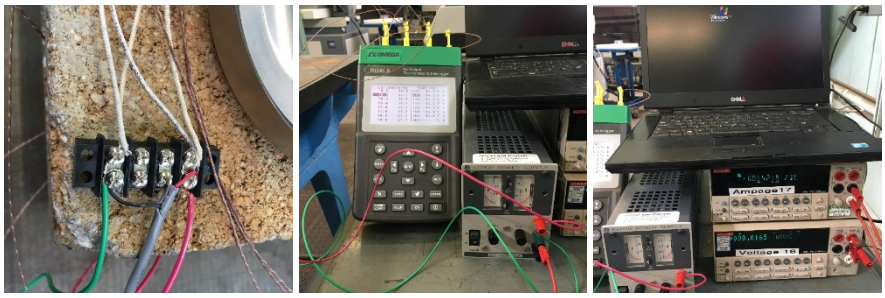

(a) (b) (c)

Figure 3 Experimental wiring setup (a) the wire connections for connecting the Hi-Temperature Cartridge Heaters to the benchtop power supply, (b) the portable thermometer and data logger, and (c) the laptop used for monitoring data trends, the benchtop power supply, and the Keithly 2000 multimeter setups that allowed for accurate voltage and amperage readings

Thermocouple locations are denoted by thermocouple 1-6, and thermocouple 7 is attached to the cart to measure the room temperature. Figures 4-6 below, show the locations as follows; thermocouple 1 = bullet header, thermocouple 2 = filter, thermocouple 3 = O-ring, thermocouple 6 = upper SAVY wall, thermocouple 5 = middle SAVY wall and thermocouple 4 = lower SAVY wall. In addition to measurement location, Figure 4 below shows the first test configuration with the bullet heater within the aluminum block alone, this configuration represents a point loading package scenario.

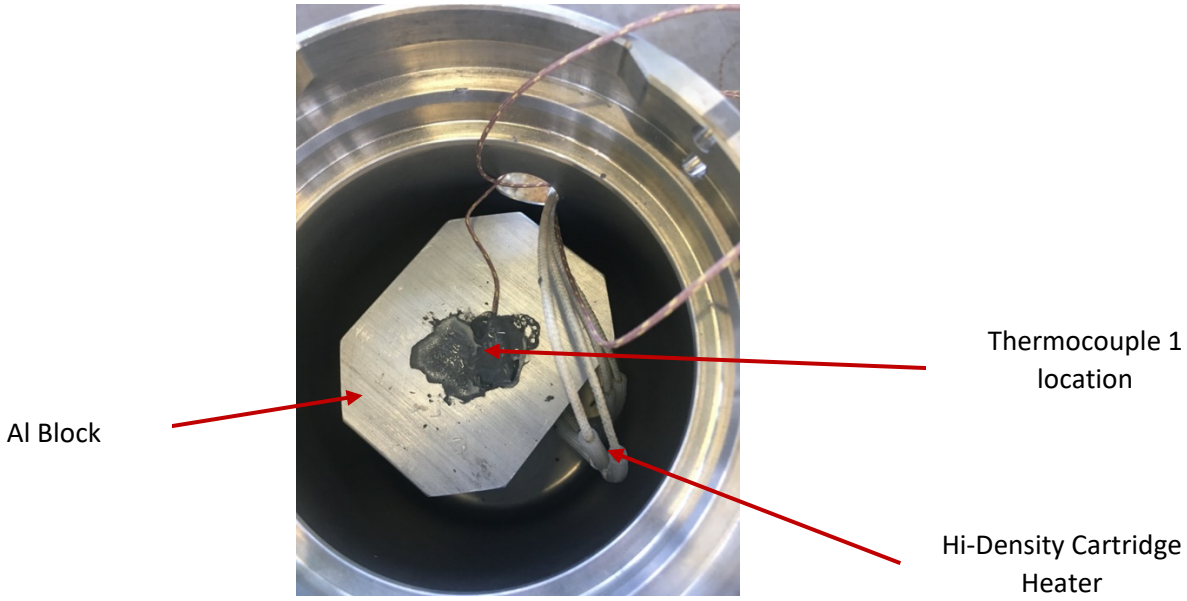

Figure 4 Thermocouple location 1 at the center of the Al block. Note: an insulating insert fills the hole for the wiring.

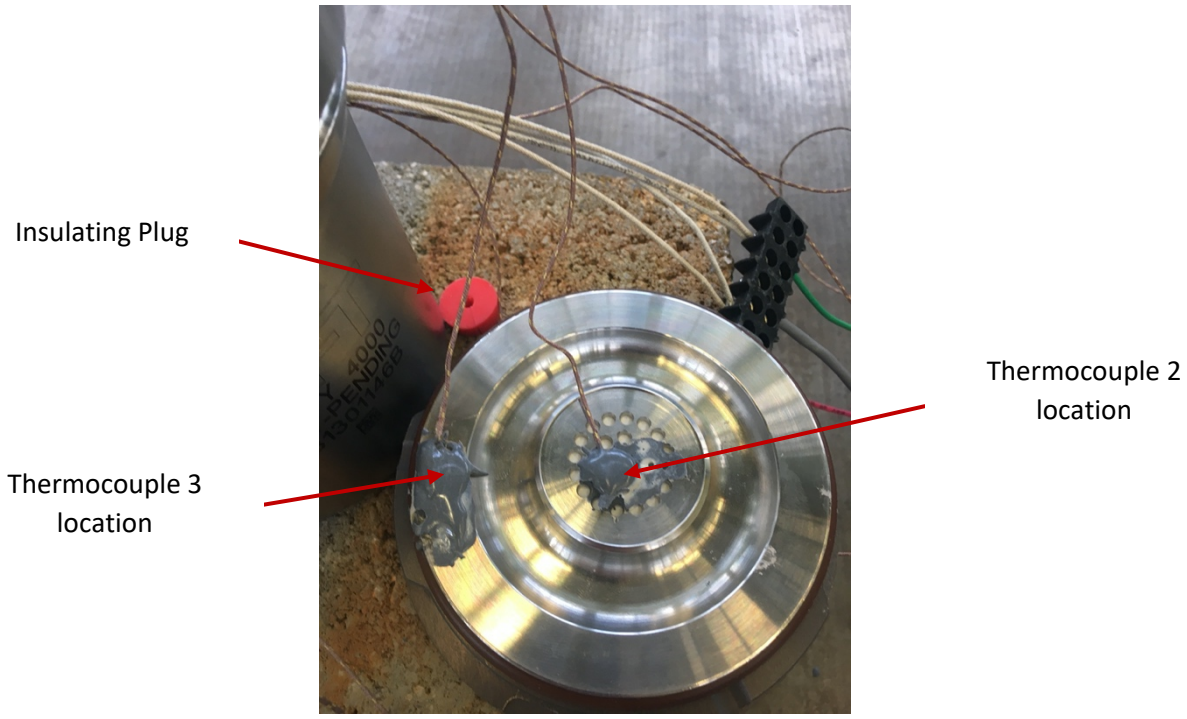

Figure 5 Thermocouple location 2 and 3. Note the insulating plug on the table beside the lid was inserted into the hole for all measurements.

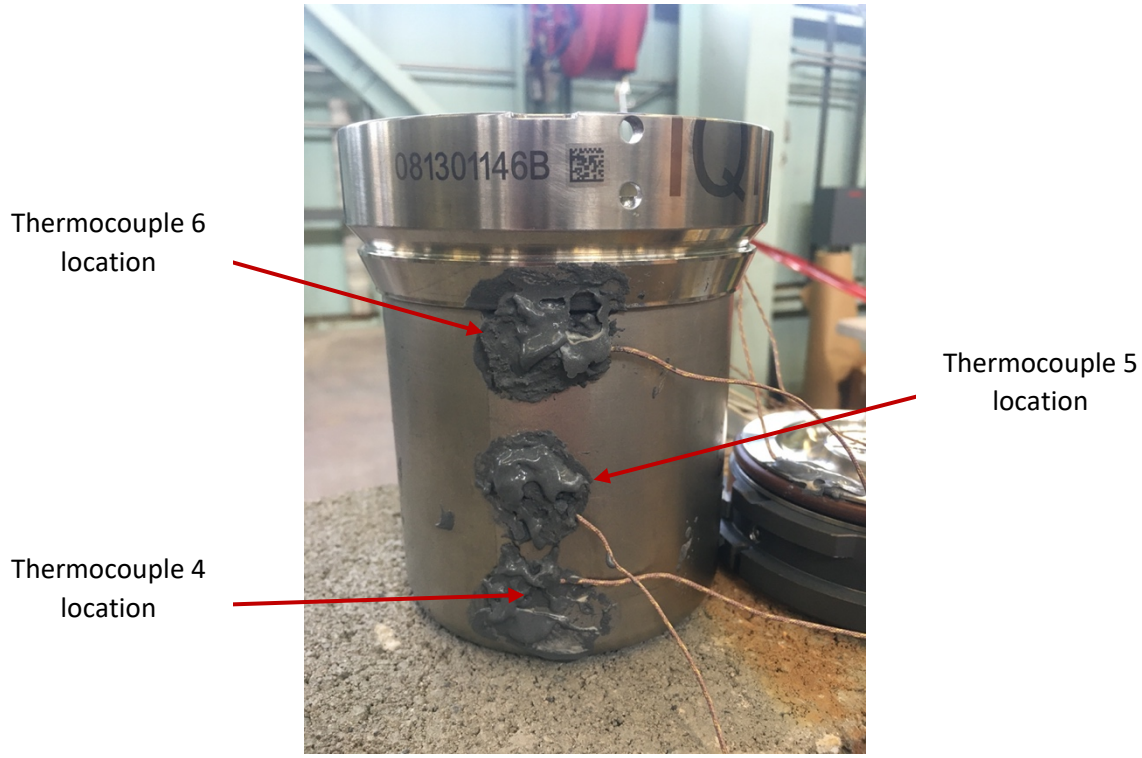

Figure 6 Thermocouple location 4-6 outside of the can

Measurements were conducted on four different configurations to capture all bounding heat load scenarios. Figure 7 below shows the different configurations used for testing. All thermocouples were in the same locations except thermocouple 1 from Figure 7 (c), which was placed in the center of the Manganin wire/copper packing conglomerate.

(a) (b) (c) (d)

Figure 7 Four tested configurations a) bullet heaters acting as a point load b) the bullet heater surrounded with copper mesh c) Manganin wire interspersed in the copper packing to further distribute the heat load d) copper mesh beneath bullet heaters to push heat load up against SAVY lid

Experimental Results

Tests were ran to steady state before recording measurements at each location. The results of the measurements conducted on the 1 quart SAVY are summarized below in Figures 8-11. Testing ranged between 20 Watts and 130 Watts and durations to reach steady state ranged from 6-24 hours. For testing beyond 60 Watts, a second benchtop power supply was used to apply enough power without violating facility safety protocols.

The first configuration represents a point loading scenario where the bullet heaters are tested alone, with no other packing material. This first configuration ranged from 20 Watts to 130 Watts with testing duration ranging from 6-24 hours to reach steady state. Figure 8 below displays the variation in measured temperatures for each test. Trending suggests the increased in power displays a linearity behavior at each location.

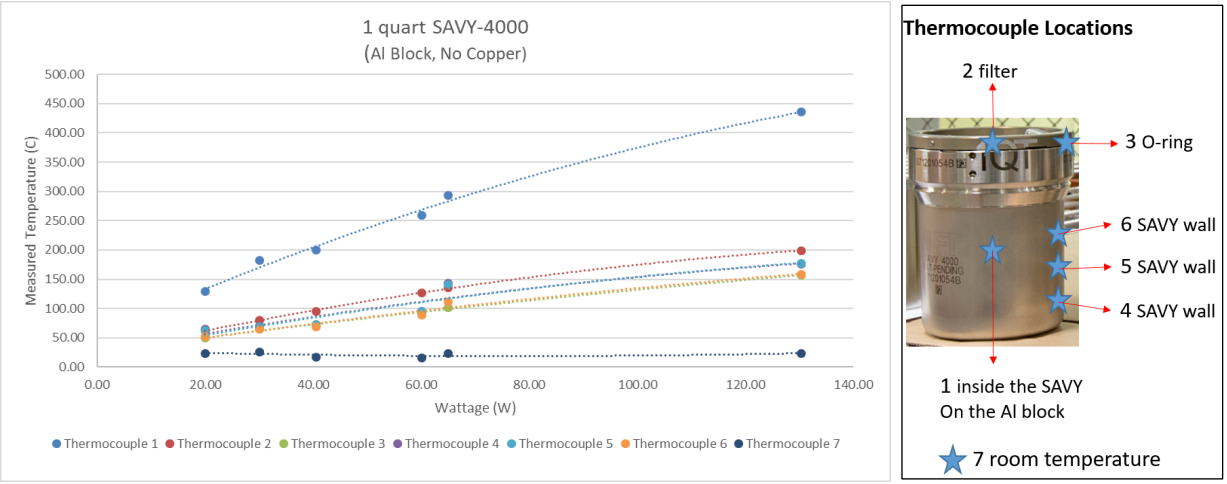

Figure 8 Thermal profile for point loading

The second configuration represents a heat distribution scenario through the addition of copper mesh surrounding the bullet heaters as seen in Figure 7 (b), better representing realistic high-heat-loaded packages. This second configuration included powers between 20 Watts and 130 Watts with testing duration also ranging 6-24 hours to reach steady state. Figure 9 below displays the temperature trend similar to the previous test run suggesting this configuration is also considered linear.

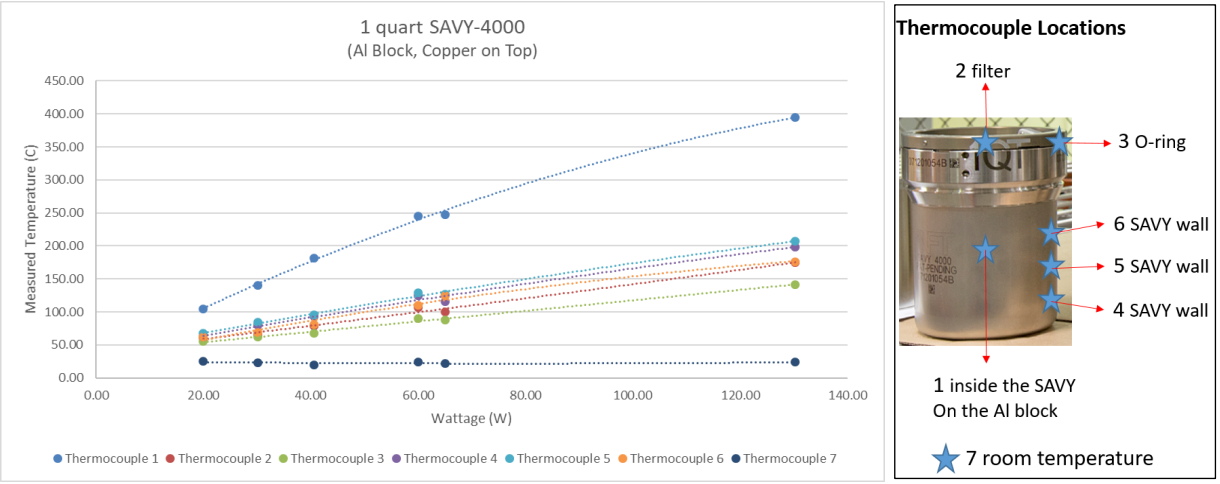

Figure 9 Thermal profile for copper mesh surrounding the bullet heater

The third configuration utilized Manganin wire to further distribute the heat within the copper mesh to achieve a balanced heat load. This third configuration was setup to ensure we can achieve a balanced distribution. The configuration can be seen in Figure 7 c). The temperatures measured at each location can be seen in Figure 10 below. The behavior is linear and correlates well with the profile seen in Figure 9 suggesting the two configurations distribute the heat in the same capacity. This configuration stopped at 60 Watts due to the compounding test runs and the Manganin becoming too hot in certain areas inside of the container and the copper mesh becoming discolored. This raised a level of concern and we did not test beyond 60 Watts.

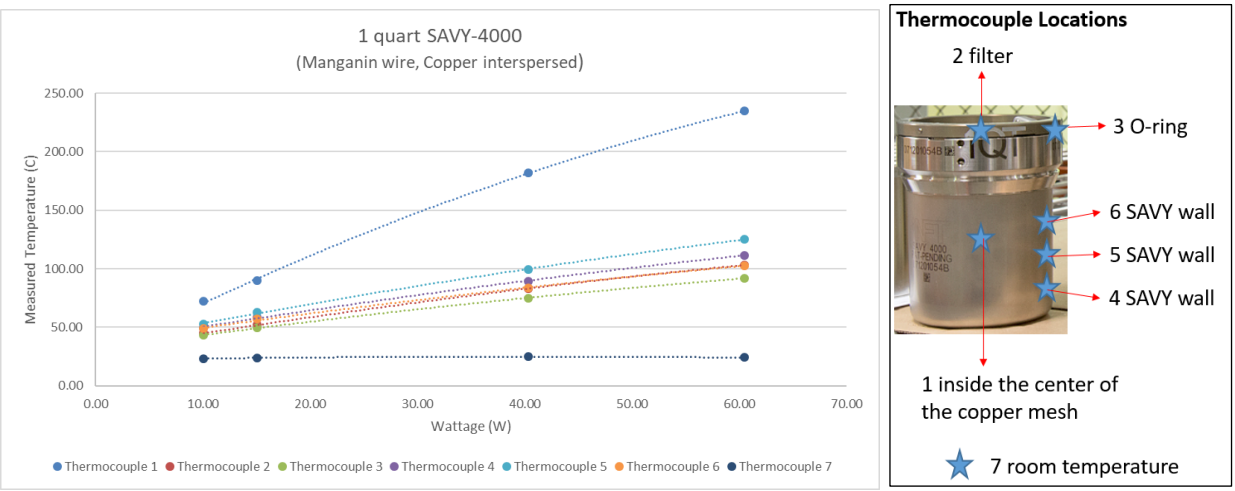

Figure 10 Thermal profile for the Manganin wire interspersed in the copper mesh

The fourth configuration consisted of using the copper mesh to push the bullet heater up against the underside of the lid, mimicking the scenario of an off balance heat distribution. This fourth configuration is considered highly unlikely. The configuration can be seen in Figure 7 (d). Figure 11 below shows the temperature measurements at each location for tests between 20 Watts and 60 Watts. Testing could not continue beyond 60 Watts due to concerns discussed in the Manganin configuration. This particular scenario poses the biggest threat toward the O-ring and filter with respect to heat loading, but this configuration is considered highly unrealistic.

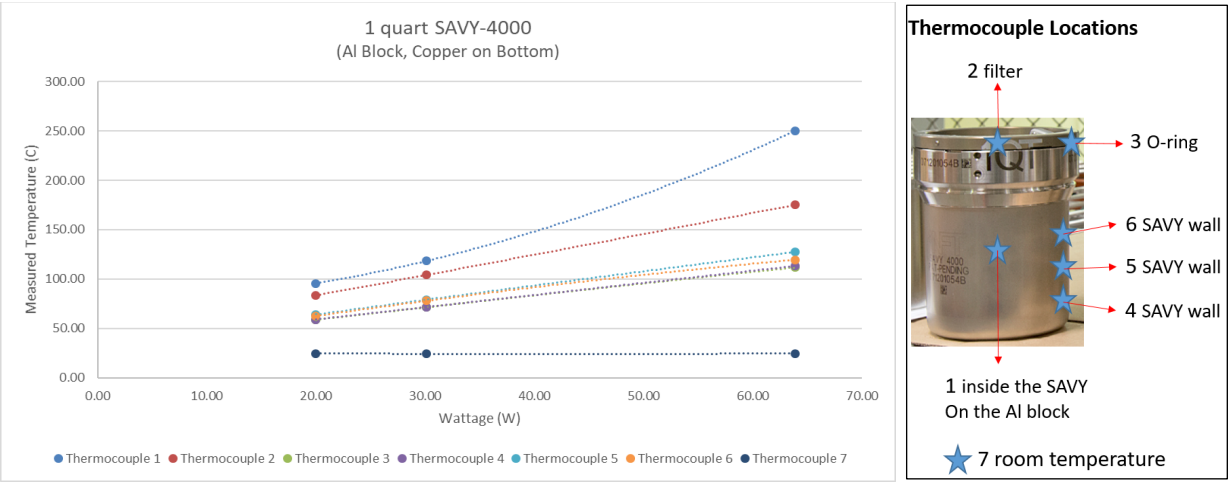

Figure 11 Thermal profile for the bullet heater up against the underside of the SAVY lid

Modeling Approach

For thermal modeling of containers, an abundance of work has been done for Pipe Overpack Containers (POC) [7,8,9] and K2 (COWS) [10] in the past. Previous testing on a POC was derived from two primary sources: the POC Handling and Operations Manual (POC-MAN-0001) and the LANL Transportation Safety Document (TSD, P&T-SA-002). Initially, LANL anticipated packing more heat source plutonium into POCs than it has previously. The SAVY-4000 is also one of many containers intended for higher heat loading investigation. While the POCs and K2 sources have been well characterized through experimental measurements and validated numerical models, work has yet to be completed for Hagan, SAVY-4000, or other storage container designs. The current effort shows the initial work completed on predicting the temperatures throughout a 1 quart SAVY container for various loadings with respect to the experimental testing.

A simplified 1 quart SAVY-4000 geometry was used for the numerical analysis conducted. Geometries were modified to remove extraneous features, such as the handle and minor air gaps present in the actual assembly. Larger air gaps were retained, particularly near the collar and locking ring. In past modeling analyses of similar nature, planes of symmetry were incorporated to simplify the modeling. Currently, a full scale analysis was conducted due to some of the geometric differences including the atypical heating block. The final de-featured 1 quart SAVY geometry was imported into ANSYS Fluent and can be seen in Figure 12 below. The de-featured geometry excludes the block geometry used to house the bullet heaters while including the internal air region of the container. A list of assumptions used for SAVY-4000 thermal modeling are provided below in Table 1.

Table 1. List of Assumptions

1.	Steady state predictions are adequate for modeling and transient effects are negligible
2.	Heat transfer coefficients will be approximated based on experimental surface temperature measurements.
3.	Heat generation provided by the bullet heater will be applied as a distributed thermal load over the block that it is housed in.
4.	SAVY handle and extraneous pins and bolts are negligible in the thermal analysis.
5.	The bottom surface of the SAVY can be treated as an adiabatic surface.

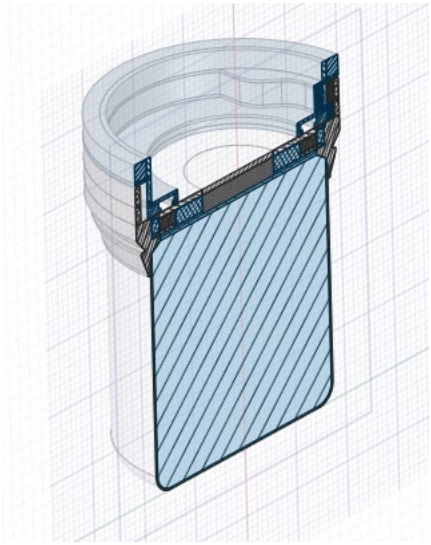

Figure 12 Sectioned view of the 1 quart SAVY with de-featured regions at the container wall, locking ring, collar and lid

The internal air region was treated as an ideal gas to capture variability in properties, specifically density, based on local temperature. To more accurately capture the variability in dynamic viscosity based upon temperature, Sutherland's law was applied to the air [11]. Steady state solutions were obtained using ANSYS FLUENT. Using computational fluid dynamics (CFD) is necessary due to the nature of the problem and presence of natural convection expected within the internal air cavity of the SAVY. In order to resolve the flow field and the heavily coupled fluid flow and heat transfer physics involved, the standard k-ϵ turbulence model developed by Launder and Sharma was used [12, 13]. Equations (1) - (3) below, highlight the Reynolds Averaged Navier-Stokes equations for turbulent kinetic energy, with turbulent dissipation and turbulent eddy viscosity:

$$\frac{\partial}{\partial t}(\rho k) + \frac{\partial}{\partial x_i}(\rho k u_i) = \frac{\partial}{\partial x_j}\left[\left(\mu + \frac{\mu_t}{\sigma_k}\right)\frac{\partial k}{\partial x_j}\right] + P_k + P_b - \rho\epsilon - Y_M + S_k \quad (1)$$

$$\frac{\partial}{\partial t}(\rho\epsilon) + \frac{\partial}{\partial x_i}(\rho\epsilon u_i) = \frac{\partial}{\partial x_j}\left[\left(\mu + \frac{\mu_t}{\sigma_k}\right)\frac{\partial \epsilon}{\partial x_j}\right] + C_{1\epsilon}\frac{\epsilon}{k}(P_k + C_{3\epsilon}P_b) - C_{2\epsilon}\rho\frac{\epsilon^2}{k} + S_\epsilon \quad (2)$$

$$\mu_t = \rho C_\mu \frac{\epsilon^2}{k} \tag{3}$$

Where ρ is the density, μ is the dynamic viscosity, k is the turbulent kinetic energy, ϵ is the turbulent dissipation, u is the velocity, P_k is the production of turbulent energy, P_b is the production of buoyancy, S is the strain rate tensor, and μ_t is the turbulent eddy viscosity. The values of $C_{1\epsilon}$, $C_{2\epsilon}$, $C_{3\epsilon}$, and C_μ are closure coefficients for the model prescribed as constant values of 1.44, 1.92, -0.33, and 0.09 respectively.

The energy equation as seen below in equation (4), was implemented to capture the conductive, convective and radiative heat transfer processes occurring. Radiative heat transfer was modeled using the P-1 model as seen in equation (5). Only gray radiation was modeled without the inclusion of any bands. Only the source/block, internal air cavity, internal container wall, and inner lid surface were included in the calculation of radiative heat transfer effects. The energy equation and P-1 radiation equation are as follows:

$$\frac{\partial}{\partial t}(\rho H_i) + \frac{\partial}{\partial x_i}(\rho u_i H_i) = \frac{\partial}{\partial x_i}\left(K \frac{\partial T}{\partial x_i}\right) + S_i \tag{4}$$

$$\frac{\partial q_r}{\partial x_i} = aG - 4an^2\sigma T^4 \tag{5}$$

Where H is the enthalpy, T is the temperature, and S is the source term. The term q_r is the radiative flux, a is the absorption coefficient, G is the incident radiation, n is the refractive index of the medium, and σ is the Stefan-Boltzmann constant [14].

The Coupled pressure-velocity solver was used to resolve the pressure and velocity fields existing within the internal air cavity of the SAVY-4000 container. A pseudo-steady state approach was applied in the iterative process. The pressure was corrected through the implementation Body Force Weighted scheme. Turbulence and the energy equations all use Second Order Upwind discretization schemes. Gravity was enabled with a reference density set to 0 g/m^3, which is standard for buoyancy driven flows.

The configuration captured for the modeling effort is based off the point loading scenario. The solution was initialized at room temperature specific to each set of experiments conducted. For heat loading values of 40.6 W, 60.1 W, and 130.2 W, with the ambient temperatures of 17.3 °C, 15.7 °C, and 23.6 °C respectively were used along the outer convective surfaces on the top and side of the SAVY. The bottom surface was treated as a perfectly adiabatic surface. Ambient air temperature applied to the convective surfaces were set according to the ambient temperatures from the experiments conducted. A heat transfer coefficient value of 5.474 W/m^2 K, 6.147 W/m^2 K, and 7.125 W/m^2 K were applied for corresponding heat loadings of 40.6 W, 60.1 W, and 130.2 W to each outer surface to mimic the expected natural convection occurring between the outer wall surface and the ambient air. Equations (6) and (7) below highlight the approach applied to determine heat transfer coefficients along the vertical side of the container [9].

$$Ra_L = Gr_L Pr = \frac{g\beta(T_S - T_\infty)L_C^3}{\nu^2} Pr \quad (6)$$

$$h = \frac{Nu_L k}{L_C} = \frac{0.59 k Ra_L^{1/4}}{L_C} \quad (7)$$

Where Ra_L is the Rayleigh number, Gr_L is the Grashof number, Pr is the Prandtl number, g is gravity, β is the inverse of the film temperature, T_s is the average surface temperature (in this study, from experiments), L_c is the characteristic length, ν is the kinematic viscosity, k is the thermal conductivity and h is the heat transfer coefficient.

The source region within the SAVY-4000 was assigned to constant heat generation rates imitating localized ^{238}Pu loading. Concentrated heat transfer payloads of 40.6 W, 60.1 W, and 130.2 W were investigated. In order to capture the three-dimensional flow effects present within the inner air cavity, the full SAVY container was modeled. For radiative boundary conditions, gray surfaces were treated with equation (8) below.

$$\frac{\partial q_{rw}}{\partial x_i} = -\frac{1}{3(a+\sigma_s) - C\sigma_s} \frac{\partial G}{\partial n_i} = \frac{4\pi e_w \frac{n^2 \sigma T_w^4}{\pi} - e_w G_w}{2(2 - e_w)} \quad (8)$$

Where σ_s is the scattering coefficient, C is the linear-anisotropic phase function coefficient, n_i is the outward normal vector and e_w is the emissivity at the wall(s). An experimentally predetermined emissivity value of 0.06 was applied to the aluminum block. The interior surface of the container and the lid was assumed to be a value of 0.189. The interior surface emissivity values for the container and the block are based upon measurements conducted. The interior surface required measurements in the current modeling iteration. Measurements made of the absorptivity are included below in Table 2. A normal emissivity value of 0.155 was determined and a correction factor of 1.218 was applied to account for the curvature along the container interior.

Table 2 SAVY Interior absorptivity measurements

Sample	12 qt SAVY Inside Surface	Sample	12 qt SAVY Inside Surface
1	0.842	7	0.846
2	0.845	8	0.841
3	0.843	9	0.845
4	0.85	10	0.844
5	0.848	11	0.845
6	0.845	12	0.847
AVE	**0.845**		
STD	**0.0025**		
Normal Emissivity	**0.155**		

Modeling Results

Figure 13 below shows the container model with its wireframe along with the various thermocouple locations used for experimental comparison. The thermocouple locations and configuration aligned with the testing locations applied for the point loading scenario as seen from Figure 4-6 mentioned above. Figures 14-16 below, display the temperature contours produced for thermal loadings of 40.6 Watts, 60.1 Watts, and 130.2 Watts with the legend corresponding to temperatures on the aluminum block within the container. Each temperature contour shows similarity in the scaling of contours with the primary deviation being the peak temperature of the block, which is inherently dependent upon the thermal loading value. It is clear, based on the thermal contours directly above the block, that Rayleigh-Bernard convection along with thermal radiation, play a crucial role in the heat transfer mechanics existing within the container interior. Based on the internal heat transfer mechanics, air is heated by the block, is propagated directly upward into the filter and then circulated outward and downward along the interior of the container wall. Air is then propelled into the side of the heated block and driven upward, continuing the cycle from the beginning. This underscores the necessity of implementing CFD into the thermal calculations and capturing the internal effects of the mass and heat flow. Additionally, given that the filter is a component that has strict thermal bounds to prevent failure, characterizing the thermal effects of the air driven from the block is crucial to predicting temperature profiles.

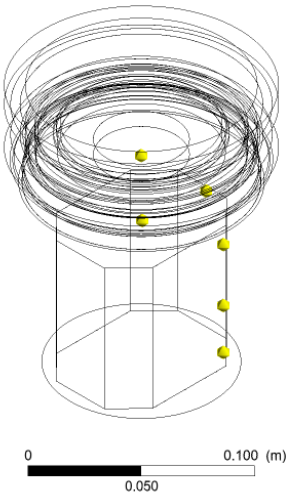

Figure 13 Thermocouple locations within the model

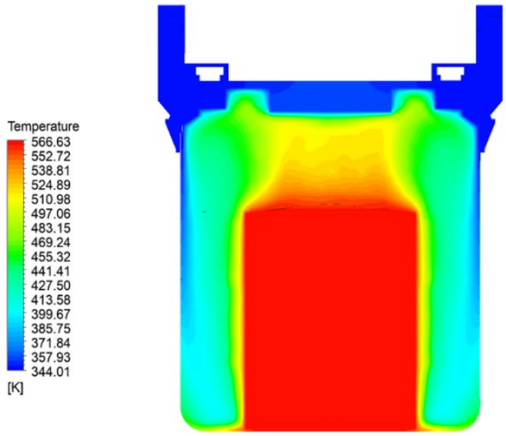

Figure 14 Temperature contours for a heat loading of 40.6 W

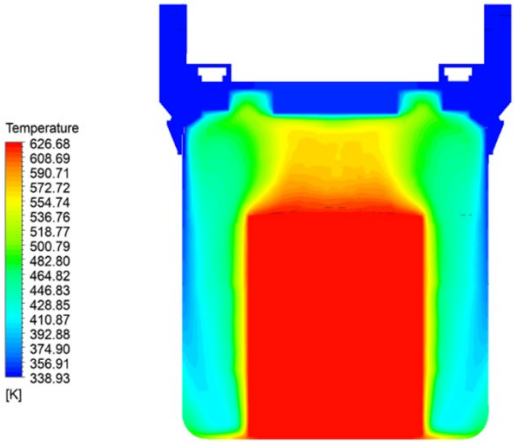

Figure 15 Temperature contours for a heat loading of 60.1 W

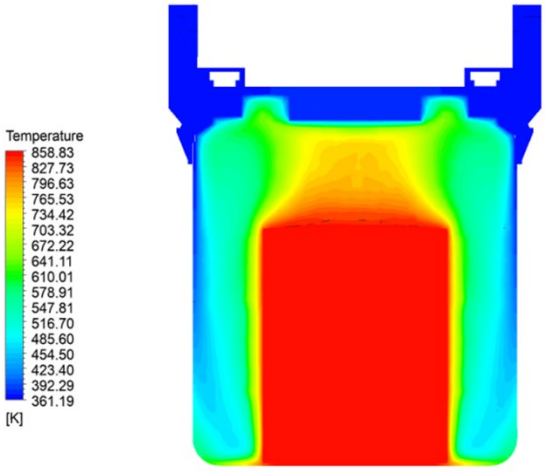

Figure 16 Temperature contours for a heat loading of 130.2 W

The raw, pseudo-steady state results for each case investigated versus the experimental values, are shown below in Table 3. The predicted values show significant deviations between the numerical and experimental work. Relative errors of 60% and higher are present for the current results. It is important

to note, the significance of thermal loading results in higher temperatures, based on equation (5) thermal radiation is to the order of T^4 and due to this relationship, it is crucial that correct emissivity values are implemented. The value applied for the aluminum block has been well defined and determined experimentally [8]. The value applied to the internal surface of the SAVY container needs to be determined experimentally in order to improve accuracy. Even with accurate emissivity values, other modes of heat transfer can cause issues in temperature predictions, such as natural convection heat transfer to the ambient and conduction through the bottom of the container. The current model still uses a constant heat transfer coefficient along the outside SAVY surfaces. Additionally, the elevated temperatures, especially at the block, may be due to an improper adiabatic surface conditions applied to the bottom where during testing, a non-negligible amount of heat is able to dissipate out of the container and into the cinder block/table that the SAVY rests on. Closer examination of the temperature contours in Figures 14-16 shows that there is a significant gradient existing along the inner boundary for the higher wattage heat loads, so there may be some human error present, given that a small shift in thermocouple location can result in a significant change in temperature predictions.

Table 3 Experimental and numerical results comparisons

Wattage	Experimental				Numerical				Error
40.60	Voltage	46.1	Amperage	0.9					
Thermocouple	Temperature		Net Temp		Temperature	Units	Net Temp	Units	Rel. Error (%)
1	200.10	°C	182.80	°C	293.48	°C	293.33	°C	60.46
2	95.20	°C	77.90	°C	112.86	°C	112.71	°C	44.69
3	72.00	°C	54.70	°C	101.21	°C	101.06	°C	84.75
4	73.10	°C	55.80	°C	125.35	°C	125.20	°C	124.37
5	72.50	°C	55.20	°C	100.00	°C	99.85	°C	80.89
6	68.70	°C	51.40	°C	82.06	°C	81.91	°C	59.36
7	17.30	°C	17.30	°C	17.30	°C	17.30	°C	0.00
60.08	Voltage	56.2	Amperage	1.1					
Thermocouple	Temperature		Net Temp		Temperature		Net Temp		Rel. Error (%)
1	258.70	°C	243.00	°C	353.52	°C	337.67	°C	38.96
2	126.90	°C	111.20	°C	121.31	°C	105.46	°C	5.16
3	92.30	°C	76.60	°C	103.45	°C	87.60	°C	14.36
4	94.70	°C	79.00	°C	142.55	°C	108.70	°C	37.59
5	95.00	°C	79.30	°C	93.89	°C	78.04	°C	1.59
6	88.80	°C	73.10	°C	76.21	°C	60.36	°C	17.43
7	15.70	°C	15.70	°C	15.70	°C	15.70	°C	0.00
130.24	Voltage	81.7	Amperage	1.6					
Thermocouple	Temperature		Net Temp		Temperature		Net Temp		Rel. Error (%)
1	435.30	°C	411.70	°C	624.65	°C	527.16	°C	28.04

2	199.00	°C	175.40	°C	221.12	°C	143.05	°C	18.44
3	156.80	°C	133.20	°C	185.45	°C	116.55	°C	12.50
4	175.60	°C	152.00	°C	215.73	°C	119.70	°C	21.25
5	176.70	°C	153.10	°C	167.57	°C	97.07	°C	36.60
6	158.80	°C	135.20	°C	140.61	°C	99.59	°C	26.34
7	23.60	°C	23.60	°C	23.60	°C	23.60	°C	0.00

Figure 17 below, shows the Yplus contours along the block surface within the SAVY-4000 for the 130.2 W thermal loading. The 130.2 W loading serves as a bounding case for the solution space. In order to capture the viscous sub-layer of the turbulent boundary layer and fully capture flow separation effects, the Yplus value along the wall needs to be ≤ 1.0 along the wall. Based on the bounding case, the peak Yplus value observed along the block and container wall where peak separation occurs is 0.28. This indicates that the internal flow within the SAVY container is well characterized and flow specific physical effects are being accurately captured. It also indicates that the inaccuracies existing between the numerical predictions and experimental measurements are driven entirely by the thermal radiation mechanics.

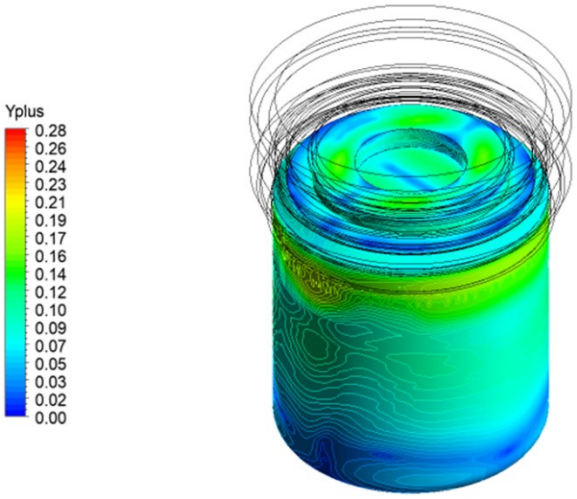

Figure 17 Yplus contours for a heat loading of 130.2 W

Modeling Conclusion

Preliminary simulations of thermal loading within a 1 quart SAVY container were conducted at loadings of 40.6 W, 60.1 W, and 130.2 W with respect to the point loading configuration. Significant relative error currently exists due to the solution dependence on thermal radiation and prescribed emissivity values along the block surfaces and the interior container wall surfaces. Yplus contours in Figure 17 for the bounding 130.2 W case showed that a peak value of 0.28 was captured along the interior surfaces, effectively providing confidence that the flow effects captured internally are accurate.

With the updated emissivity values determined experimentally, errors between measurements are still substantial. A variable heat transfer coefficient along the outer surface is necessary. Additionally, the bottom surface of the SAVY, cannot be treated as an adiabatic surface: meaning that there is some non-negligible heat that is dissipating through the bottom surface into the table/cinder block that the SAVY is

sitting on during testing. Additionally, some human error is likely present in the temperature predictions due to the high temperature gradients that exist along the inner surface and the placement of the thermocouples. The issues that are present in the predicted values were diminished in previous studies due to insulation that existed which minimized the variables of heat dissipation as well as minimizing the effects of the external boundary conditions on the steady state solution [7].

The current model can provide an overly conservative estimate of expected temperatures due to less heat being allowed to dissipate outward given the current boundary conditions; however, the model will not be able to accurately predict temperatures within 5-10% error for all locations in the same manner that previous iterations were able to provide with more insulated containers (i.e. Pipe Overpack Containers, K2's). This modeling effort suggests that any thermal characterization of SAVY containers must rely heavily on thermal testing to decide what temperatures would be expected and to ensure that temperature limitations are not exceeded.

Conclusion

The goal of the study was to investigate thermal loading beyond the 25 Watt limit and measure the steady state temperatures at various locations on the container body and key components such as the filter and the Viton O-ring. Testing was accomplished by utilizing a 1 quart SAVY-4000 container that is considered bounding for all other sizes due to having the smallest volume for heat loading materials. Components and location of interest include: filter, O-ring, aluminum block housing of the bullet heaters, various locations on the container wall and a location outside the container to measure ambient room temperature. Heat loadings between 20 Watts and 130 Watts were observed for each configuration presented. The four configurations were implemented to bound all loading scenarios, with only two configurations reaching 130 Watts. From the four configurations, the last configuration with the bullet heater pushed up against the underside of the lid is unrealistic and shall not be viewed as a configuration to base new Wattage limits. The first three configurations provide high confidence in bounding all loading scenarios from a worst case of point loading to two different disbursement configurations. Results show from the worst case scenario (point loading) at 130 Watts, the filter experienced a thermal loading of 200 °C and the O-ring of 156.8 °C at steady state. The next step is to correlate these measurements with previous studies on lifetime extension to express a lifetime expectancy of these measured temperatures. All three realistic configurations shall continue to be used in future thermal testing of the SAVY-4000 series.

Modeling efforts have been initiated and shown to be challenging, capturing predictions from the current configurations. Challenges facing this effort are: capturing the variable heat transfer coefficient along the container wall, a better representation of the adiabatic floor the container sits on and the continued emissivity measurements on the current 1 quart SAVY that will correspond to the SAVY's specific fabrication finish. The current model has prediction errors with respect to the experimental values upwards of 60% error on some locations. The error is on the high side where the model tends to over predict values and can be considered highly conservative. The error present is driven predominantly by using an improper assumption, item 5 in Table 1, that the bottom of the container is adiabatic similar to the modeling approach applied for POCs. A non-negligible amount of heat is exiting through the bottom surface of the container and into the cinder block, resulting in elevated source temperatures. Additionally, oxidation is occurring when 130 W loadings are applied, causing alterations in the emissivity values within the container. Although the model is over predicting, it is in the best

interest to continue running tests with different configurations to capture more data to continue to refine the model for accuracy. As the project stands, decisions shall rely on physical testing for thermal measurements until the model is progressed further. Future modeling will need to account for the alterations in emissivity for oxidation at higher heat loadings and include appropriate boundary conditions at the bottom surface of the container or the inclusion of material to represent the test apparatus the container is sitting on.

The next phase of the project will include continued thermal testing that mimic's container storage. The storage configuration will depict shelving with numerous containers in an array, with each container loaded with bullet heaters and thermocouples at various locations. The thermal loading scenarios should reflect the loading sequence in this report with further analysis on the temperatures profiles at key components with correlation on lifetime expectancy. Modeling will continue to progress with additional testing to refine predictions and to complement further thermal testing.

References

1. DOE M 441.1-1, Nuclear Material Packaging Manual, Office of ES&H, DOE, on-line at www.directives.doe.gov/directives-documents
2. Anderson L. K., M. W. Blair, E. J. Hamilton, E. J. Kelly, M. E. Moore, P. H. Smith, T. A. Stone, J. G. Teague, D. K. Veirs, E. W. Weis and T. F. Yarbro (2013) "Safety Analysis Report for the SAVY 4000 Container Series, Revision 3." LA-CP-13-01502, Los Alamos National Laboratory.
3. Jung, J.G., William S., Approval of Design Life Extension for the SAVY-4000 Container Series (U1900606). 2019, US Department of Energy, National Nuclear Security Administration, Los Alamos Field Office.
4. Omega. "Ready-Made Insulated Thermocouples with Kapton, PFA Glass Braid Insulation and Molded Connectors. https://www.omega.com/en-us/temperature-measurement/temperature-wire-sensors/5lsc-5srtc/p/SC-GG-K-30-36
5. Omega. "8-Channel Portable Thermometer/Data Logger with SD Card Data Recorder." Data sheet. https://www.omega.com/en-us/temperature-measurement/temperature-and-humidity-data-loggers/p/RDXL8-Series
6. Tempco. "Preconfigured and Stock Hi-Density Cartridge Heaters." https://www.tempco.com/Tempco/Resources/Part-Numbers/Hi-Density-Cartridge-Heater-Preconfigured-Part-Numbers.htm
7. J. Oka, T. Stone, P. Smith, M. Caviness, M. Croce, P. Santi, J. Riglin and J. Tafoya, "Steady State Thermal Analysis of the Pipe Over Pack Container for Transuranic Waste at Los Alamos National laboratory," Los Alamos, November 2016.
8. J. Riglin, J. Oka, M. Croce, M. Caviness, P. Carson and D. Thorp, "Thermal Characterization and Modeling of Pipe Overpack Containers for Concentrated Transuranic Waste Storage; LA-UR-18-24881," in INMM Conference Proceedings, Baltimore, MD, 2019.
9. R. R. Geinitz, D. T. Thorp and M. A. Rivera.United States Patent US5998800A, 1998.
10. J. Oka, J. Riglin and A. Nettleton, "Thermal dissipation studies and Pu238/Li source simulation (MCNP) of the K2 containers (COWS); LA-UR-18-29955," LANL, Los Alamos, NM, 2018.
11. W. Sutherland, "The viscosity of gases and molecular force," Philosophical Magazine, vol. 5, no. 36, pp. 507-531, 1893.
12. B. E. Launder and B. I. Sharma, "Application of Energy Dissipation Model of Turbulence to the Calculation of Flow Near a Spinning Disc," Letters in Heat and Mass Transfer, vol. 1, no. 2, pp. 131-138, 1974.
13. D. C. Wilcox, Turbulence Modeling for CFD, Anaheim: DCW Industries, 1998.
14. S. S. Sazhin, E. M. Sazhina, O. Faltsi-Saravelou and P. Wild, "The P-1 model for thermal radiation transfer: advantages and limitations," Fuel, vol. 75, no. 3, pp. 289-294, 1996.
15. Y. Cengel, Heat and Mass Transfer: A Practical Approach, New York, NY: McGraw-Hill, 2007.